MAGNETIC RESONANCE IN MEDICINE 17, 357–367 (1991)

Measurement of the Blood–Brain Barrier Permeability and Leakage Space Using Dynamic MR Imaging. 1. Fundamental Concepts

PAUL S. TOFTS AND ALLAN G. KERMODE

Multiple Sclerosis NMR Research Group, Institute of Neurology, Queen Square, London WC1N 3BG, United Kingdom

Received June 14, 1989; revised December 27, 1989

Leakage of Gd-DTPA through a defective blood–brain barrier is measured quantitatively using dynamic MRI scanning, in which repeated scans are made after a bolus injection. Image registration artifacts are minimized; a dose of 0.1 mM/kg and an IR sequence enable enhancement to be measured quantitatively. The triexponential enhancement curve is fitted to a theoretical model based on compartmental analysis. The transfer constant, or permeability surface area product per unit volume of tissue (k), and leakage space per unit volume of tissue (v_l) are measured. Estimates for a quickly enhancing multiple sclerosis lesion are $k = 0.050$ min^{-1}, $v_l = 21\%$; for a slow one $k = 0.013$ min^{-1}, $v_l = 49\%$. This implies permeability in the range 4–17 $\times 10^{-6}$ cm s^{-1}, in broad agreement with other physiological methods. The method is noninvasive and can be used to make serial measurements in patients and in experimental animal models. The time course of pathological aspects of diseases with blood–brain barrier breakdown, such as multiple sclerosis, tumors, and infections (e.g., HIV) can be studied, along with their response to therapy. The measurements are of physiological variables and are therefore independent of imaging equipment and field.

INTRODUCTION

Gd-DTPA scanning has been used extensively to identify areas of blood–brain barrier (BBB) breakdown in neurological disease (*1–3*). Generally this work has tended to ask the binary question Is there enhancement? rather than the quantitative question How much enhancement is there? The question of when the optimum time is to scan for maximum sensitivity has also received little attention. This paper presents two novel additions to standard Gd-DTPA imaging. First we describe dynamic scanning, which enables a curve of signal enhancement versus time to be produced, with a consequent differentiation between lesions that enhance with different time courses. Second we describe a quantitative analysis of the dynamic curve which enables absolute measurements of blood–brain barrier permeability and leakage space to be made. This is likely to be useful in the study of all conditions of the central nervous system in which the blood–brain barrier is disturbed, e.g., multiple sclerosis, tumors, and infections (including HIV). A subsequent paper (part 2) will describe practical issues (e.g., variation in the Gd-DTPA plasma concentration between individuals; optimum scanning times and sequences; and experience from scanning large numbers of patients). The compartmental analysis described is applicable to DTPA attached to any label and can be used equally well in other imaging modalities. We have already presented

0740-3194/91 $3.00

preliminary accounts of dynamic Gd imaging (*4, 5*) and measurements of permeability surface area product and leakage space (*6, 7*).

MODEL

The model consists of two parts: first we use a compartmental model to establish the time course of the Gd-DTPA tracer concentration in the tissue; second we relate that to observed MRI signal enhancement.

Tracer Concentration in Tissue

A compartmental model for DTPA is used to model the concentration of tracer with time. It consists (Fig. 1) of a plasma volume, connected to a large extracellular space which is distributed throughout most of the body (e.g., muscle), but does not occur in the brain (where the BBB surrounds the capillary vessels). The kidneys drain tracer from the plasma, and hence from the extracellular space. We have modified this model by adding a fourth compartment, the lesion, which is connected to the plasma through a leaky membrane. This compartment is small enough not to influence the overall plasma concentration. We assume a bolus (i.e., short) injection of the tracer into the plasma, and fast mixing within the plasma. Implicit in this (and any) compartmental model is the assumption that all tracer within the compartment is well mixed; in particular this means that capillary flow in the lesion must be high enough to prevent the plasma concentration from being locally depleted by leakage of the tracer through the blood–brain barrier.

The plasma curve (i.e., the time course of tracer concentration in the plasma) can be derived theoretically (Appendix I), and is a biexponential decay:

$$C_p(t) = D\{a_1\exp(-m_1t) + a_2\exp(-m_2t)\}. \quad [1]$$

D is the DTPA dose (mM/kg body wt); a_1 and a_2 are the amplitudes of the components and m_1 and m_2 are their rate constants. The fast component (a_1, m_1) corresponds to

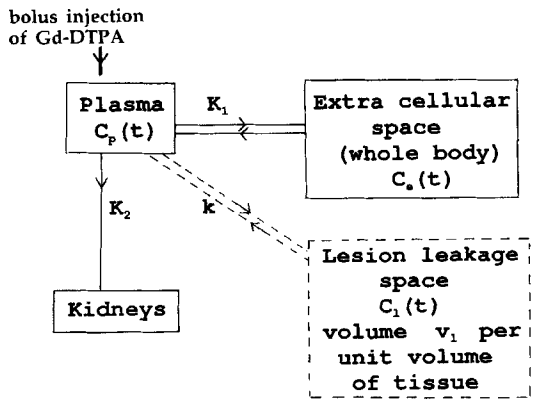

FIG. 1. Compartmental model of DTPA tracer distribution. The conventional compartments (plasma, whole-body extracellular space, and kidneys) are represented within solid lines. We have modified the model by adding leakage through the blood–brain barrier to a "lesion leakage space" (dotted lines).

equilibration between plasma and extracellular space (which are relatively well connected); the slow component (a_2, m_2) corresponds to emptying of these two well-coupled compartments to the kidneys. The corresponding decay times are

$$\tau_1 = 1/m_1; \qquad \tau_2 = 1/m_2, \tag{2}$$

respectively. The analytic calculation of the amplitudes and decay constants is straightforward only under the condition that $K_1 \gg K_2$ (i.e., that the plasma compartment is much better connected to the extracellular space than to the kidneys); in this case approximate solutions are given by Eqs. [A6] and [A8].

This biexponential solution has been confirmed by several experimenters using Tc-DTPA (*8, 9*) and Gd-DTPA (*10*). The data of Weinmann *et al.* (*10*), for a dose of 0.25 mM/kg, were fitted to Eq. [1], and parameters $a_1 = 3.99$ kg/liter, $a_2 = 4.78$ kg/liter, $m_1 = 0.144$ min^{-1}, $m_2 = 0.0111$ min^{-1} obtained (see Fig. 2). These parameters were used to characterize the plasma curve in the subsequent analysis. The rate constants correspond to decay times $\tau_1 = 6.9$ min, $\tau_2 = 90$ min.

The lesion (i.e., area of defective BBB) is modeled as containing a leakage space which is defined as that part of the tissue, in the lesion, to which the plasma tracer has access. For example, it might consist of a small space around each capillary, or it might be the extracellular space in the lesion. The amount of tracer in the leakage space is $v_l V_t C_l$, where v_l is the fraction of lesion tissue which the leakage space occupies ($0 \leqslant v_l < 100\%$); V_t is the lesion tissue volume and C_l is the tracer concentration in the leakage space. The flow of tracer from plasma into the leakage space is then

$$v_l V_t \frac{dC_l}{dt} = PS(C_p - C_l). \tag{3}$$

P is the permeability coefficient; S is the surface area of leaking membrane. We have assumed, in using the concept of permeability coefficient, that flow is proportional to

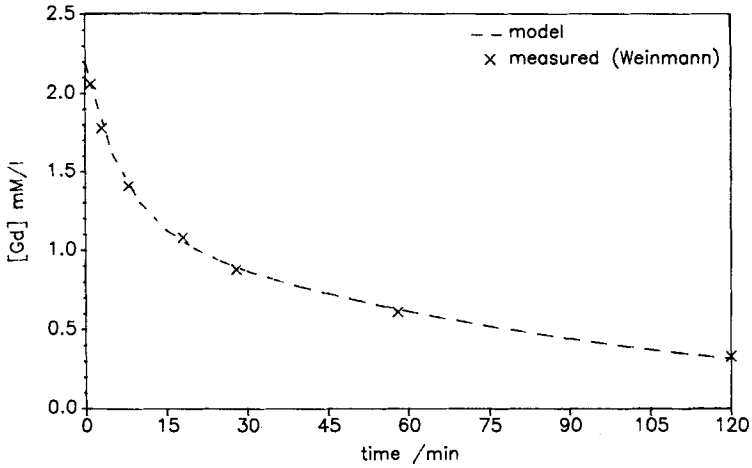

FIG. 2. Biexponential plasma concentration curve, following a bolus injection of 0.25 mM/kg. Data from Weinmann *et al.* (*10*) are shown fitted to a biexponential curve (Eq. [1]). Values of the fitted parameters are given in the text.

the area of leaking membrane and to the concentration difference across the membrane. Equation [3] may be written as

$$v_l \frac{dC_l}{dt} = k(C_p - C_l), \qquad [4]$$

where $k = PS/V_t$ is the permeability surface area product per unit volume of tissue, or transfer coefficient, with units of [min^{-1}] (*11*). Our Eq. [4] differs slightly from the conventional one used to describe the transport of a tracer across a cell membrane (*11*). In the latter case, all of the volume inside the cell is available to the tracer, and $v_l = 1$ and does not appear in the equation. The physical meaning of k can also be understood by considering the response to a step increase in plasma concentration, from zero to a constant value C_p at time zero. The solution to Eq. [4] is then $C_t(t) = C_p(1 - \exp(-kt/v_l))$, and k/v_l is the rate constant for filling of the leakage space.

The leakage space concentration C_l can now be calculated from Eqs. [1] and [4]. The solution (Appendix II) is a triexponential. MRI signal enhancement is dependent on the mean concentration in the lesion tissue, C_t. Since no signal enhancement is seen in normal white matter, we can ignore the contribution to C_t from plasma Gd and consider only the contribution of the leakage space Gd to total tissue Gd. Therefore

$$C_t = v_l C_l \qquad [5]$$

and we obtain, from Eq. [A10],

$$C_t(t) = D\{b_1\exp(-m_1t) + b_2\exp(-m_2t) + b_3\exp(-m_3t)\}, \qquad [6a]$$

where

$$\begin{aligned} m_3 &= k/v_l; \qquad b_1 = ka_1/(m_3 - m_1); \\ b_2 &= ka_2/(m_3 - m_2); \qquad b_3 = -(b_1 + b_2) \end{aligned} \qquad [6b]$$

and a_1, a_2, m_1, m_2 have been determined empirically from the plasma curve. The initial slope of the curve, from Eqs. [1], [4], and [5], is

$$\frac{dC_t(0_+)}{dt} = kD(a_1 + a_2). \qquad [7]$$

By using different values of k and v_l we can generate families of $C_t(t)$ curves from Eq. [6]. For a given leakage space, Fig. 3a shows that increasing permeability increases the initial slope of the concentration, as expected from Eq. [7]. Increased permeability also decreases the time to maximum enhancement. For fixed permeability (Fig. 3b) increasing leakage space has no effect on the initial slope, but does affect the maximum concentration reached and delays the time to peak enhancement.

MRI Signal

The increases in relaxation rates are linearly related to Gd concentration in the tissue

$$\frac{1}{T_1} = \frac{1}{T_{10}} + R_1C_t; \qquad \frac{1}{T_2} = \frac{1}{T_{20}} + R_2C_t, \qquad [8]$$

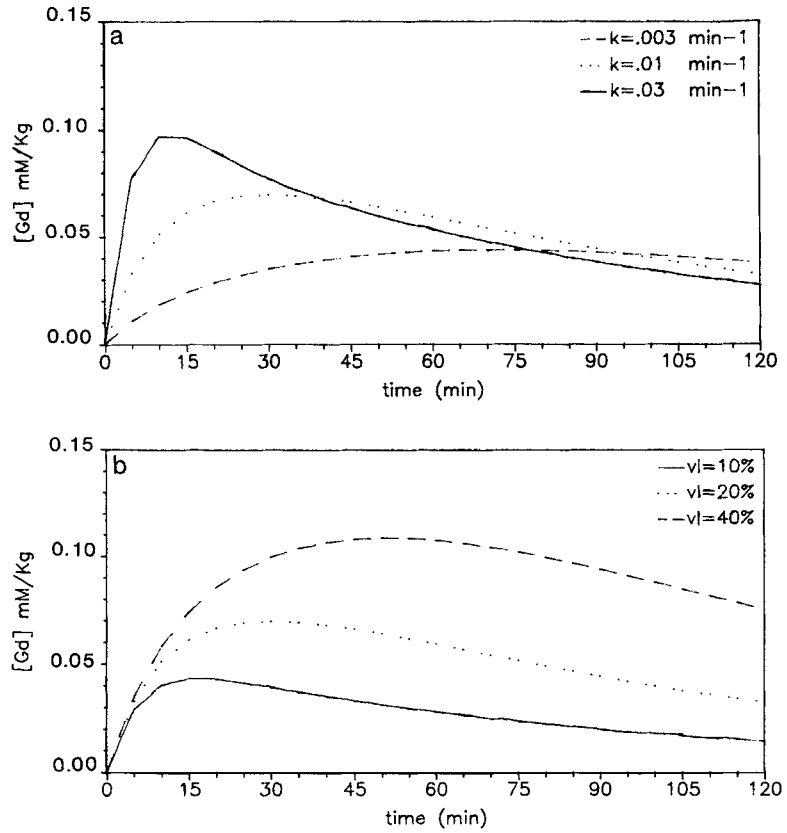

FIG. 3. Model triexponential lesion concentration curves, following a bolus injection of 0.1 mM/kg of Gd-DTPA. (a) Fixed leakage space v_l = 20%, varying permeability k. (b) Fixed permeability k = 0.01 min^{-1}, varying leakage space v_l.

where R_1 = 4.52 s^{-1} mM^{-1}liter; R_2 = 5.66 s^{-1}mM^{-1}liter at 0.5 T (*12*). T_{10}, T_{20} are the relaxation times before injection of Gd; T_1, T_2 are the values after injection. The preinjection T_1 is measured using a conventional IR/SE pair;

$$S_{SE0} = N_H \exp(-T_E/T_{20})(1 - \exp(-T_R/T_{10})) \quad [9a]$$

$$S_{IR0} = N_H \exp(-T_E/T_{20})(1 - 2\exp(-T_I/T_{10}) + \exp(-T_R/T_{10})), \quad [9b]$$

where S_{SE0}, S_{IR0} are the signal intensities. The ratio of signals gives T_{10}. With appropriate care of the instrumental aspects of data collection, measured relaxation times are within 5% of true values (*13*). Postinjection IR signal is measured as a function of time:

$$S_{IR}(t) = N_H \exp(-T_E/T_2)(1 - 2\exp(-T_I/T_1) + \exp(-T_R/T_1)) \quad [10a]$$

$$= S_{IR0} \exp(-T_E R_2 C_t(t))$$

$$\times \left(\frac{1 - 2\exp(-T_I(T_{10}^{-1} + R_1 C_t(t))) + \exp(-T_R(T_{10}^{-1} + R_1 C_t(t)))}{1 - 2\exp(-T_I T_{10}^{-1}) + \exp(-T_R T_{10}^{-1})\}} \right). \quad [10b]$$

Note that in Eq. [10b] we have taken full account of changes in T_2 caused by the presence of Gd, even though no explicit measurement of T_2 was made.

For a particular k and v_l the $C_t(t)$ curve is known (Eq. [6]) and therefore the $S_{IR}(t)$ curve can be computed. This is least squares fitted to the measured $S_{IR}(t)$ curve to obtain estimates of k and v_l.

IMAGING PROCEDURE

For dynamic scanning to be performed, patient movement must be carefully restricted. An indwelling catheter is placed in the cubital vein, before the patient is placed in the scanner. A movement restriction device is used to help cooperative patients keep still during the examination (*14, 15*). The patient is scanned with a T_2-weighted multislice sequence (e.g., $SE_{2000/60}$ at 0.5 T) to locate regions of high T_2, where BBB permeability may be raised. Over this region a multislice IR/SE combination (e.g., $IR_{1000/40/500}$ and $SE_{1000/40}$) gives the T_1 of the lesions. Gd-DTPA (0.1 mM/kg) is injected into the catheter over a period of 1 min with the patient remaining still and repeated IR scans are made. $IR_{1000/40/500}$ T_1-weighted scans are preferred to the conventional $SE_{500/40}$, since their increased T_R reduces slice profile errors in the measurement of T_1 (*16*).

A dose of 0.1 mM/kg was used in order to keep on that part of the signal versus $1/T_1$ curve where signal is still rising with $1/T_1$. At the higher dose of 0.2 mM/kg, where signal enhancement is greater, accuracy is actually worse because relaxation rates may be so high that signal is independent of relaxation rate (i.e., the system relaxes completely between pulses). Lesions then lose their visible structure and attain a uniform, toothpaste-like appearance (*4*).

Since the permeability can be obtained from the initial slope of the $C_t(t)$ curve (Eq. [7]), if leakage space v_l does not need to be estimated it is necessary only to scan for about 10–20 min postinjection.

PATIENT MEASUREMENTS

Preliminary data are shown in Fig. 4 for a rapidly and a slowly enhancing multiple sclerosis lesion scanned at 0.5 T. The patient was a 23-year-old female with clinically definite multiple sclerosis (*17*). Both lesions were known to be less than 3 months old from previous MRI scans. Repeat $IR_{1020/40/500}$ scans at approximately 6-min intervals were carried out, up to 105 min after injection, with a 20-min break for rest. The regions of interest were approximately 1.3 cm^2 in size in a 5-mm-thick slice. Unfortunately, for this patient it was not possible to measure T_1 before injection of Gd-DTPA, and therefore this was estimated using a mean value (646 ms) from measurements on other patients (*3*). The fitted values were $k = 0.050$ min^{-1}, $v_l = 21\%$ for the rapidly enhancing lesion and $k = 0.013$ min^{-1}, $v_l = 49\%$ for the slowly enhancing lesion. The estimated preinjection T_1 value is subject to an error of about ±20% (2 SD) (*3*); propagation of this error gives uncertainty of about ±40% (2 SD) in the estimated parameters k and v_l. Another data set, collected for 24 min after accurate measurement of preinjection T_1, gave estimates for eight lesions for k in the range 0.014–0.074 min^{-1}.

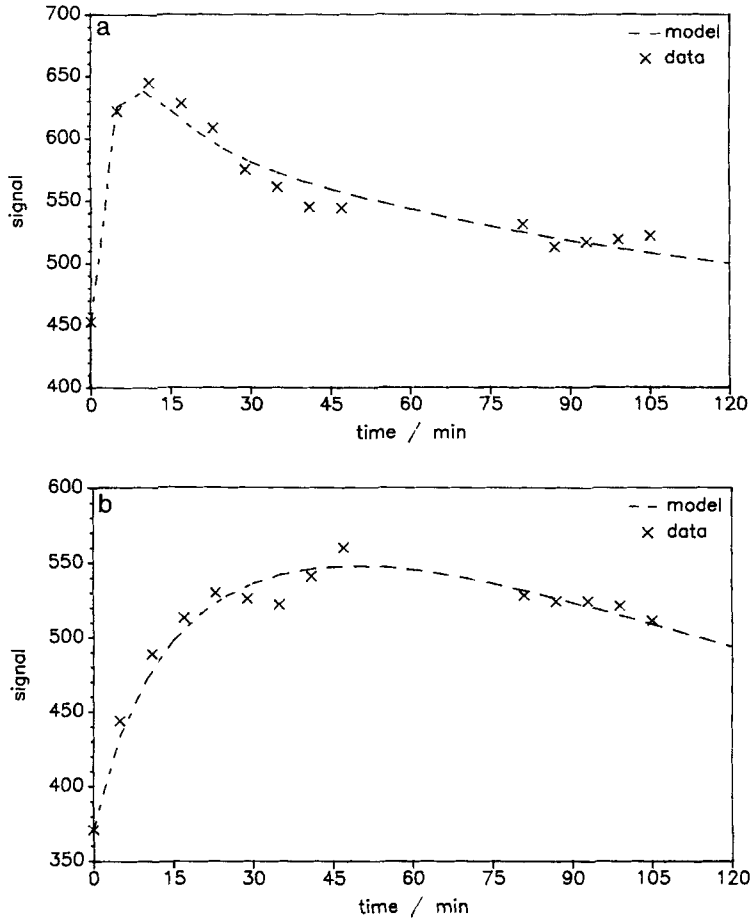

FIG. 4. Signal enhancement (IR1020/40/500) after injection of 0.1 mM/kg Gd-DTPA at time zero into a patient with active multiple sclerosis. The broken lines are fitted curves. (a) A rapidly enhancing lesion k = 0.050 min^{-1}, v_l = 21%. (b) A slowly enhancing lesion k = 0.013 min^{-1}, v_l = 49%.

DISCUSSION

These measurements of permeability surface area product per unit volume are the first to be made using any imaging modality that is truly noninvasive (we consider the use of ionizing radiation in CT and PET to be invasive). The compartmental analysis presented here, showing the time course of tracer concentration in the lesion in response to a bolus injection, is applicable to all imaging modalities, not specifically MRI. Measurements of various transfer and rate constants have been made using PET with [^{68}Ga]EDTA (*18–20*) and $^{82}Rb^+$ (*21, 22*). Our transfer constant k is equal to the influx constant K_i used by Iannotti *et al.* (*19*) and Pozzilli *et al.* (*20*), although our model includes reflux from the lesion back to the plasma. PET measurements are however limited by the poor spatial resolution obtainable (approximately 10 mm) and therefore severely underestimate the permeability of small lesions (*7*). In large

lesions we expect that PET and MRI values will be similar. Normal transfer constants are too low to measure with MRI (since no Gd-DTPA enhancement is seen in normal white matter (*3*)); with PET a value of 3×10^{-4} min^{-1} was obtained (*19*). X-ray computed tomography observation of I-DTPA has been used to visualize areas of defective BBB (*23*); however, the signal enhancement is poor, the radiation dose high, and it is unlikely to be quantitative. Physiologists have traditionally measured permeability in animal models by using a continuous infusion of tracer to provide an approximately constant plasma concentration (*11, 24, 25*). After a specified time the animal is sacrificed, the brain is sliced, and the concentration of tracer in the brain is measured. Our method has two advantages over all those mentioned above: (1) the need for continuous infusion and monitoring of the plasma concentration is eliminated by mathematical modeling of a bolus injection and (2) the measurement of tracer concentration is noninvasive and therefore can be used for serial measurements in animal models (*26*) and for measurements in humans. Dynamic MRI is thus the method of preference for noninvasive measurement of abnormally high BBB permeability to medium-sized molecules such as DTPA.

Five assumptions are implicit in our model. First we have assumed perfect mixing, i.e., that the capillary blood flow is sufficient to replenish loss of tracer into the lesion. Peak flow of tracer from the plasma is kC_pV_t (from Eqs. [3], [4]) at time zero, when $C_e = 0$. Replenishment of plasma tracer by capillary flow is $pFC_p\rho V_t$, where p is the fraction of blood that is plasma, F is the blood flow, and ρ is the tissue density. Our assumption is therefore equivalent to

$$pF\rho \gg k. \qquad [11]$$

The left-hand side of this inequality has a value of at least 0.40 min^{-1} (assuming $p = 50\%$, $F \geq 80$ ml/100 g tissue/min (*11*), $\rho = 1.04$ g/ml); therefore the highest value of k that we have measured (0.074 min^{-1}) is unlikely to significantly deplete the plasma concentration. However, if blood flow was to be abnormally low, or if permeability was to be higher than our highest measured value, then plasma depletion might become significant, and we may measure a transfer constant k that is limited by capillary blood flow. In the limit of an infinitely large leak in the BBB we would expect to measure an effective permeability determined by the rate at which tracer could reach the lesion through the capillaries, i.e., by blood flow. Since we have measured an average transfer coefficient over the volume of interest, it is possible that local values exceed this.

Second we have assumed that all tracer which leaks into the lesion will eventually return to the plasma, once tracer has cleared from the plasma. In fact we have observed diffuse signal enhancement in parts of lesions up to 5 h after injection (*5*); this observation suggests that several hours after injection other mechanisms may become manifest. Slow diffusion may be responsible for transporting tracer to the site of signal enhancement, and clearance may be to the cerebrospinal fluid, rather than back to the plasma. We expect these effects to be insignificant in data collected during the first hour after injection.

Third we have assumed tracer flow is linearly related to concentration difference across the BBB; this assumption is implicit in any measurement of permeability. It could be verified in animal models by giving a preinjection of unlabeled DTPA and

looking for any perturbation to the measured permeability. Any nonlinear transfer mechanism which might saturate at high levels of DTPA would thus be detected.

Fourth we have assumed that the partition coefficient between plasma and leakage space is unity, i.e., that at equilibrium $C_p = C_l$. A partition coefficient different from unity is unlikely given that the solvent is water in both compartments. The permeabilities in each direction have also been assumed equal, which is likely to be the case for a nonelectrolyte (*11*).

Fifth we have assumed all patients have the same plasma curve. The Gd dose given is proportional to body weight, so most of the variation between individuals will be removed. Weinmann *et al.* (*10*) found the normal variation in plasma concentrations to be 10–15%, for a fixed dose per body weight; therefore this variation is unlikely to be a large source of error. More accurate curves could perhaps be produced by monitoring the plasma concentration after injection, either by imaging in the choroid plexus (where there is no blood–tissue barrier) or by taking serial blood samples and subsequently imaging these. Patients with impaired renal function will require different data analysis. PET measurements of BBB permeability usually measure the plasma curve explicitly, using arterial sampling, and then perform a numerical integration in place of the analytic solution given in the appendices.

The quantity k that we have measured is the permeability surface area product per unit volume, or transfer coefficient, although in places we have loosely referred to it as permeability, for convenience. The surface area of capillary per unit volume is known to be approximately 50 cm^2/g (*24*) for white matter. From this we calculate true permeability values for our two multiple sclerosis lesions to be in the range 4–17 $\times 10^{-6}$ cm s^{-1}. These are comparable to the permeability values for similarly sized molecules measured by traditional (i.e., non-PET) means. Skeletal muscle capillary has a permeability to sucrose and Cr-EDTA in the range 5–23 $\times 10^{-6}$ cm s^{-1} (*24, 27*); the choroid plexus has a permeability to creatanine of 5×10^{-6} cm s^{-1} (*24*). Juhler *et al.* (*25*) have measured permeability–surface area products (i.e., transfer constants) for ^{3}H-sucrose in Experimental Allergic Encephalomyelitis (a model of Multiple Sclerosis); they obtained values of the order of 0.003 min^{-1}, which is consistent with our slowly leaking lesion. Recently Larsson *et al.* (*28*) have measured in acute multiple sclerosis a rate constant (EF/λ) which appears to equal k/v_l and obtained values in the range 0.04–0.11 min^{-1}. The method requires catheterization for the measurement of Gd concentration in blood samples. These rate constants are similar to our values of k/v_l (0.03–0.24 min^{-1}). Our leakage space measurements are in agreement with those made in our group of extracellular space using biexponential analysis of magnetization decay curves (20–60%), suggesting that the Gd-DTPA leakage space is in fact the extracellular space.

APPENDIX I: DERIVATION OF PLASMA CURVE

Flow from plasma to extracellular space and kidneys is

$$-V_p \frac{dC_p}{dt} = K_1(C_p - C_e) + K_2 C_p, \qquad [A1]$$

where K_1 and K_2 are constants describing the flow rate per unit concentration difference,

with units [ml/min], V_p is the plasma volume, and C_e is the tracer concentration in the extracellular space. Flow into the extracellular space (volume V_e) is

$$V_e \frac{dC_e}{dt} = K_1(C_p - C_e). \qquad [A2]$$

Eliminating C_e gives

$$V_p V_e \frac{d^2C_p}{dt^2} + (K_2V_e + K_1V_e + K_1V_p)\frac{dC_p}{dt} + K_1K_2C_p = 0. \qquad [A3]$$

The solution to this second-order linear differential equation is a biexponential decay for C_p (*29*):

$$C_p(t) = A_1\exp(-m_1t) + A_2\exp(-m_2t). \qquad [A4]$$

A_1 and A_2 are constants which can be determined from the initial conditions; m_1 and m_2 are rate constants which are equal to the roots of Eq. [A3] ($m_1 > m_2$). The general solution for m_1 and m_2 is tedious and opaque; however, we have prior knowledge that the coupling between the plasma and the extracellular spaces is much stronger than that between plasma and kidneys (since the interfacing surface area is much larger in the former case); i.e.,

$$K_1 \gg K_2 \qquad [A5]$$

and the solution to [A3] is then

$$m_1 = K_1(V_p + V_e)/V_pV_e; \qquad m_2 = K_2/(V_p + V_e). \qquad [A6]$$

The initial conditions, immediately after the bolus injection, are

$$C_p(0_+) = D/V_p; \qquad C_e(0_+) = 0 \qquad [A7]$$

and using [A1], [A4], and [A5] we obtain

$$a_1 = A_1/D = V_e/(V_p(V_p + V_e)); \qquad a_2 = A_2/D = 1/(V_p + V_e). \qquad [A8]$$

APPENDIX II: DERIVATION OF LESION CURVE

Equations [1] and [4] can be rewritten as

$$\frac{dC_l(t)}{dt} + m_3C_l(t) = m_3D(a_1\exp(-m_1t) + a_2\exp(-m_2t)), \qquad [A9]$$

where $m_3 = k/v_l$. This first-order linear differential equation in $C_l(t)$ has the solution (*29*)

$$C_l(t) = D\left(\frac{m_3a_1}{m_3 - m_1}\exp(-m_1t) + \frac{m_3a_2}{m_3 - m_2}\exp(-m_2t) + c\exp(-m_3t)\right), \qquad [A10]$$

where c is a constant which can be determined from the initial condition $C_l(0_+) = 0$.

ACKNOWLEDGMENTS

We are grateful to Dr. Clive Hawkins for many helpful discussions, to Miss Caroline Persaud for assistance in the preparation of this manuscript, and to Professor Ian McDonald for his constant encouragement. The

Multiple Sclerosis NMR Research Group is supported by the Multiple Sclerosis Society of Great Britain and Northern Ireland, and the Medical Research Council of Great Britain. Gd-DTPA was provided by Schering AG.

REFERENCES

1. D. G. GADIAN, J. A. PAYNE, D. J. BRYANT, I. R. YOUNG, D. H. CARR, AND G. M. BYDDER, *J. Comput. Assist. Tomogr.* **9,** 242 (1985).
2. R. I. GROSSMAN, F. GONZALES-SCARANO, S. W. ATLAS, S. GALETTA, AND D. H. SILBERBERG, *Radiology* **161,** 721 (1986).
3. D. H. MILLER, P. RUDGE, G. JOHNSON, B. E. KENDALL, D. G. MACMANUS, I. F. MOSELEY, D. BARNES, AND W. I. MCDONALD, *Brain* **111,** 927 (1988).
4. A. G. KERMODE, P. S. TOFTS, W. I. MCDONALD, AND D. MACMANUS, "Society of Magnetic Resonance in Medicine 7th Annual Meeting, Works-in-Progress," p. 21, 1988.
5. A. G. KERMODE, P. S. TOFTS, D. G. MACMANUS, B. E. KENDALL, D. P. E. KINGSLEY, I. F. MOSELEY, E. P. G. H. DU BOULAY, AND W. I. MCDONALD, *Lancet* **2,** 1203 (1988).
6. P. S. TOFTS AND A. G. KERMODE, *Magn. Reson. Imaging* **7**(Suppl 1), 150 (1989).
7. P. S. TOFTS AND A. G. KERMODE, *J. Neurol. Neurosurg. Psych.* **52,** 1019 (1989).
8. H. L. ATKINS, K. G. CARDINALE, W. C. ECKELMAN, W. HAUSER, J. F. KLOPPER, AND P. RICHARDS, *Radiology* **98,** 674 (1971).
9. J. G. MCAFEE, G. GANGE, H. L. ATKINS, P. T. KIRCHNER, R. C. REBA, M. D. BLAUFOX, AND E. M. SMITH, *J. Nucl. Med.* **20,** 1273 (1979).
10. H. J. WEINMANN, M. LANIADO, AND W. MÜTZEL, *Phys. Chem. Phys. Med. NMR* **16,** 167 (1984).
11. H. DAVSON, K. WELCH, AND M. B. SEGAL, *in* "Physiology and Pathophysiology of the Cerebrospinal Fluid," pp. 36–38, Churchill Livingstone, Edinburgh, London, Melbourne, & New York, 1987.
12. H. J. WEINMANN, R. C. BRASCH, W. R. PRESS, AND G. E. WESBEY, *AJR* **142,** 619 (1984).
13. G. JOHNSON, I. E. C. ORMEROD, D. BARNES, P. S. TOFTS, D. G. MACMANUS, *Brit. J. Radiol.* **60,** 143 (1987).
14. P. S. TOFTS, A. G. KERMODE, D. G. MACMANUS, AND W. H. ROBINSON, "Society of Magnetic Resonance in Medicine 8th Annual Meeting, p. 611, 1989.
15. P. S. TOFTS, A. G. KERMODE, D. G. MACMANUS, AND W. H. ROBINSON, *J. Comput. Assist. Tomogr.* **14,** 163 (1990).
16. I. R. YOUNG, D. J. BRYANT, AND J. A. PAYNE, *Magn. Reson. Med.* **2,** 355 (1985).
17. C. M. POSER, D. W. PATY, L. SCHEINBERG, W. I. MCDONALD, F. A. DAVIS, G. C. EBERS, K. P. JOHNSON, W. A. SIBLEY, D. H. SILBERBERG, W. W. TOURTELLOTTE, *Ann. Neurol.* **13,** 227 (1983).
18. R. A. HAWKINS, M. E. PHELPS, S.-C. HUANG, J. A. WAPENSKI, P. D. GRIMM, R. G. PARKER, G. JUILLARD, AND P. GREENBERG, *J. Cereb. Blood Flow Metabol.* **4,** 507 (1984).
19. F. IANNOTTI, C. FIESCHI, B. ALFANO, P. PICOZZI, L. MANSI, C. POZZILLI, A. PUNZO, G. DEL VECCHIO, G. L. LENZI, M. SALVATORE, AND P. CONFORTI, *J. Cereb. Blood Flow Metabol.* **11,** 390 (1987).
20. C. POZZILLI, S. BERNARDI, L. MANSI, P. PICOZZI, F. IANNOTTI, B. ALFANO, L. BOZZAO, G. L. LENZI, M. SALVATORE, P. CONFORTI, AND C. FIESCHI, *J. Neurol. Neurosurg. Psych.* **51,** 1058 (1988).
21. D. J. BROOKS, R. P. BEANEY, A. A. LAMMERTSMA, K. L. LEENDERS, P. L. HORLOCK, M. J. KENSETT, J. MARSHALL, D. G. THOMAS, AND T. JONES, *J. Cereb. Blood Flow Metabol.* **4,** 535 (1984).
22. J. O. JARDEN, V. DHAWAN, A. POLTORAK, J. B. POSNER, AND D. A. ROTTENBERG, *Ann. Neurol.* **18,** 636 (1985).
23. E. S. SEARS, A. MCCAMMON, R. BIGELOW, AND L. A. HAYMAN, *Neurology* **32,** 815 (1982).
24. M. BRADBURY, *in* "The Concept of a Blood–Brain Barrier," Wiley, New York, 1979.
25. M. JUHLER, D. I. BARRY, H. OFFNER, G. KONAT, L. KLINKEN, AND O. B. PAULSON, *Brain Res.* **302,** 347 (1984).
26. C. P. HAWKINS, P. M. G. MUNRO, F. MACKENZIE, J. KESSERING, P. S. TOFTS, E. P. G. H. DU BOULAY, D. N. LANDON, AND W. I. MCDONALD, *Brain* **113,** 365 (1990).
27. C. CRONE AND D. LEVITT, *in* "Handbook of Physiology, Section 2: The Cardiovascular System" (E. M. Renkin and C. C. Michel, Eds.), Vol. IV(1), American Physiological Society, Bethesda, 1984.
28. H. B. W. LARSSON, M. STUBGAARD, J. L. FREDERIKSEN, M. JENSEN, O. HENRIKSEN, AND O. PAULSON, "Society of Magnetic Resonance in Medicine 8th Annual Meeting," p. 744, 1989.
29. M. L. BOAS, "Mathematical Methods in the Physical Sciences," Wiley, New York, 1966.